We are IntechOpen, the world's leading publisher of Open Access books Built by scientists, for scientists

4,800
Open access books available

122,000
International authors and editors

135M
Downloads

Our authors are among the

154
Countries delivered to

TOP 1%
most cited scientists

12.2%
Contributors from top 500 universities

CLARIVATE ANALYTICS BOOK CITATION INDEX INDEXED

WEB OF SCIENCE™

Selection of our books indexed in the Book Citation Index in Web of Science™ Core Collection (BKCI)

Interested in publishing with us?
Contact book.department@intechopen.com

Numbers displayed above are based on latest data collected.
For more information visit www.intechopen.com

27

Heading Measurements for Indoor Mobile Robots with Minimized Drift using a MEMS Gyroscopes

Sung Kyung Hong and Young-sun Ryuh
Dept. of Aerospace Engineering, Sejong University
Korea
Center for the Advanced Robot Industry,
Korea Institute of Industrial Technology
Korea

1. Introduction

Autonomous cleaning robots increasingly gain popularities for saving time and reduce household labor. Less expensive self-localization of the robot is one of the most important problems in popularizing service robot products. However, trade-offs exist between making less expensive self-localization systems and the quality at which they perform. Relative localizations that utilize low-cost gyroscope (hereafter refer to as a gyro) based on technology referred to as Micro Electro-Mechanical System (MEMS) with odometry sensors have emerged as standalone, and robust to environment changes (Barshan & Durrant-Whyte, 1995; De Cecco, 2003; Jetto et al., 1995). However, the performance characteristics associated with these low-cost MEMS gyros are limited by various error sources (Yazdi et al., 1998; Chung et al., 2001; Hong, 1999). These errors are subdivided into two main categories according to their spectral signature: errors that change rather rapidly (short-term) and rather slowly (long-term) (Skaloud et al., 1999). Due to these error sources, the accumulated angular error grows considerably over time and provides a fundamental limitation to any angle measurement that relies solely on integration of rate signals from gyros (Hong, 2003; Stilwell et al., 2001).
Currently, because of their potential for unbounded growth of errors, odometry and gyro can only be used in conjunction with external sensors that provide periodic absolute position/attitude updates (Barshan & Durrant-Whyte, 1995; De Cecco, 2003; Jetto et al., 1995). However, such aiding localization schemes not only increase installation and operating costs for the whole system, but also only lead to compensation of the long-term inertial errors. That is, the angle deterioration due to quickly changing errors (system noise, vibration) is not detectable by external sensors over a short time period (Sun et al., 2005; Hong, 2008a). Considering this concept, better performance of a localization system can be expected if short-term noise in the gyro signal is suppressed prior to integration. In the previous study (Hong, 2008a; Hong & Park, 2008b), it has been shown that the threshold

filter is very effective for suppression the broadband noise components at the gyro output. However, the threshold filter was partially effective only when there's no turning motion.
To improve our previous studies and achieve further minimized drift on yaw angle measurements, this chapter examines a simple, yet very effective filtering method that suppresses short-term broadband noise in low cost MEMS gyros. The main idea of the proposed approach is consists of two phases; 1) threshold filter for translational motions, and 2) moving average filter for rotational motions to reject the broadband noise component that affects short-term performance. The switching criteria for the proposed filters are determined by the motion patterns recognized via the signals from the gyro and encoder. Through this strategy, short-term errors at the gyro signal can be suppressed, and accurate yaw angles can be estimated regardless to motion status of mobile robots. This method can be extended to increase the travel distance in-between absolute position updates, and thus results in lower installation and operating costs for the whole system.
An Epson XV3500 MEMS gyro (Angular Rate Sensor XV3500CB Data sheets, 2006) was selected as the candidates at our lab. It has performance indexes of 35°/hr bias stability, 3.7°/√hr ARW(Angle Random Walk). These specifications are saying that, if we integrate the signals of this gyro for 30 minutes (assumed cleaning robot's operating time) it can be supposed to have the standard deviation of the distribution of the angle drift up to 20°, which provides a fundamental limitation to any angle measurement that relies solely on integration of rate. However, experimental results with the proposed filtering method applied to XV3500 demonstrate that it effectively yields minimal-drift angle measurements getting over major error sources that affect short-term performance.
This chapter is organized as follows. Section 2 describes the error characteristics for the gyro XV3500. In Section 3, the algorithms for minimal-drift heading angle measurement including self-identification of calibration coefficients, threshold filter, and moving average filter are presented. In Section 4, the experimental results are provided to demonstrate the effectiveness of the proposed method. Concluding remarks are given in Section 5.

2. The error characteristics of a MEMS gyro

In general, gyros can be classified into three different categories based on their performance: inertial-grade, tactical-grade, and rate-grade devices. Table 1 summarizes the major requirements for each of these categorizes (Barbour & Schmidt, 2001).
The MEMS gyros, Epson XV3500, used in this research are of a quality that is labeled as "rate grade" devices. This term is used to describe these sensors because their primary application is in the automotive industry where they are used for active suspension and skid control via rate measurement, not angle measurement. Therefore it is normally considered that to estimate precise angle with unaided (without odometer/velocity or GPS or magnetometer aiding) rate-graded MEMS gyro is a quite challenging problem.
These sensors range in cost from $25 to $1000 and are expected to drop in price in the future. In this study the rate gyro that was used and tested extensively was the Epson XV3500 (shown in Figure 1) that costs less than $50.
The output of gyro has rather complex noise characteristics that are produced by many different error sources. A detailed general model and a thorough discussion on each individual error component can be found for instance in (Titterton & Weston, 2004) and references therein.

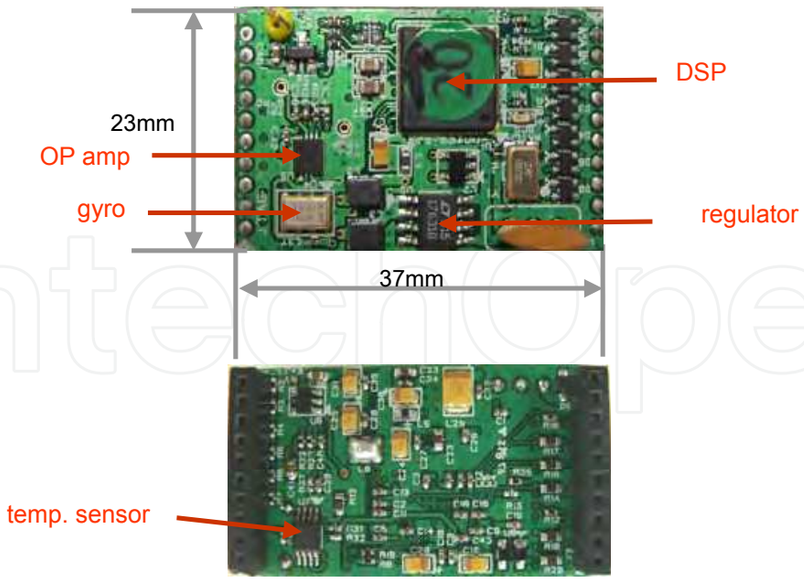

Fig. 1. Epson XV3500 gyro module

	Rate-grade	Tactical-grade	Inertial-grade
Angle Random Walk (°/√hr)	>0.5	0.5~0.05	<0.001
Bias Drift (°/hr)	10~1,000	0.1~10	<0.01
Scale Factor Accuracy (%)	0.1~1	0.01~0.1	<0.001

Table 1. Performance requirement for different type of gyros

In the following, as shown in Figure 2, gyro errors are subdivided into two main categories according to their spectral signature: errors that change rather rapidly (short-term) and rather slowly (long-term). The characteristics of two different categories can be analyzed through an Allan-variance chart. Figure 3 shows an Allan-variance chart for XV3500s. This chart is representative of all the other XV3500 gyros tested.

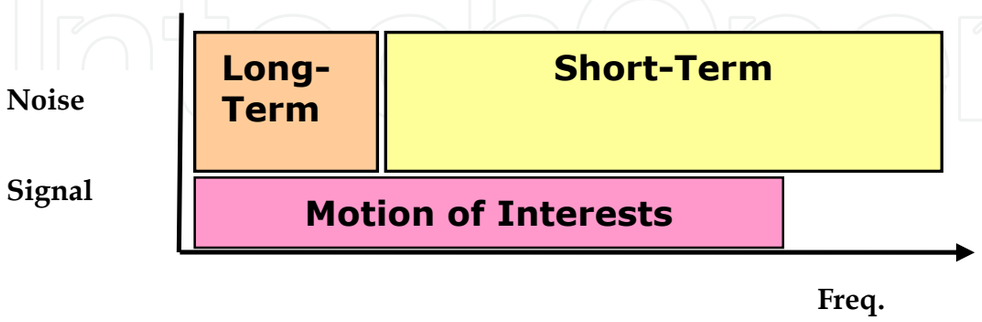

Fig. 2. A schematic plot of gyro signal in the frequency domain

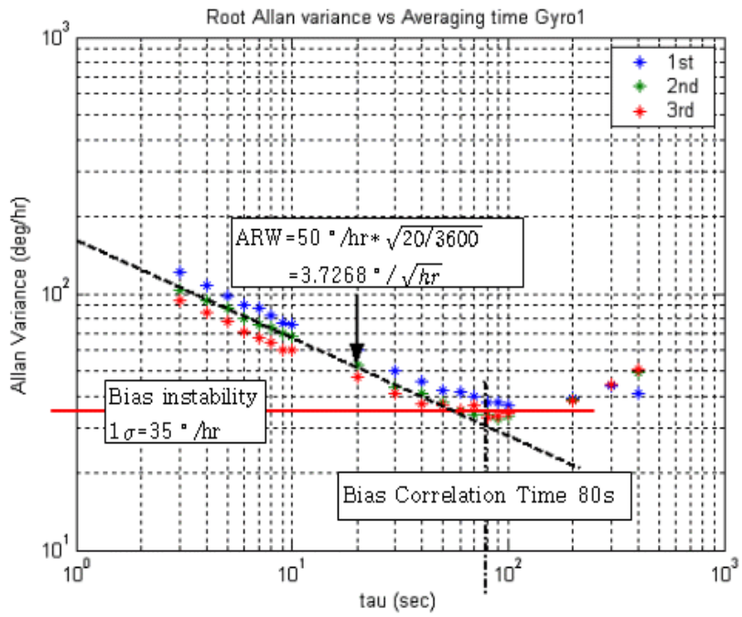

Fig. 3. Allan Variance Chart

2.1 Long-Term Errors

This category combines errors in the low frequency range. Individual error sources belonging to this category would include the main components of the gyro bias drift, scale factor, misalignment errors, and so on. From Figure 3, it is shown that the gyros exhibit a long-term instability, what is called bias instability, which tends to dominate the output error after about 200 sec. The initial upward slope of approximately +1/2 indicates that the output error in that time period is predominately driven by an exponentially correlated process with a time constant much larger than 200 sec. In Figure 3, it is shown that the mean bias instability, which is the maximum deviation of the random variation of the bias, is 35°/hr. This instability tends to dominate the long-term performance. Usually, updating gyro with some other angle reference observation or self-calibration prevents divergence due to such long-term errors.

2.2 Short-Term Errors

This category complements the long-term inertial error spectrum up to half of the gyro sampling rate. The prevailing error sources include Angle Random walk (ARW) defined as the broadband sensor noise component, and correlated noise due to vehicle vibrations. Without some other angle reference, this will be a fundamental uncertainty in the result of the angle calculation. Better performance of a system can be expected if short-term noise in the gyro is suppressed prior to integration. To a certain extent, this can be achieved by implementing optimal low pass filter beyond motion bandwidth. After two repeated experiments for 10 sets of gyros, averaged ARW was 3.7°/√hr as shown in Figure 3. This represents the short-term performance limit of XV3500 in that the standard deviation of the angle distribution obtained by integrating rate signals for an hour is 3.7 degrees

In short, we found that XV3500 as a low-cost MEMS gyro used here is dominated by three major error sources: scale-factor error (s) and bias (b) that affect long-term performance, and ARW defined as the broadband noise component (w) that affects short-term performance. We assume the output of the gyro is written

$$r_m(t) = (1+s)r(t) + b + w \tag{1}$$

where $r_m(t)$ is the measured rate from gyro and $r(t)$ is the true rate about the sensitive axis.

3. Minimal-drift yaw angle measurement

For long-term errors, as conceptually described in Figure 4, it can be reduced by periodical calibration and compensation of scale-factor error (s) and bias (b) (Hong, 2008; Hong & Park, 2008). In this chapter, a novel self-calibration algorithm is suggested for improved long-term performance.

For short-term errors (ARW and vibration), most of the signal processing methodologies currently employed utilize Kalman filtering techniques to reduce the short-term error and to improve the estimation accuracy. Unfortunately, the convergence of these methods (the time to remove the effect of the short-term error and to provide an accurate estimate) during the alignment processes can take up to 15min. In addition to their time-consuming algorithms, these techniques are complex to design and require a considerable effort to achieve real-time processing. Although some modern techniques have been introduced to reduce the noise level and some promising simulation results have been presented, real-time implementation with an actual gyro has not yet been reported.

To achieve further minimized drift on yaw angle measurements, in this section, we examine a simple, yet very effective filtering method that suppresses short-term broadband noise in low cost MEMS gyros. The concept of the proposed strategy is described in Figure 4. The main idea of the proposed approach is consists of two phases; 1) threshold filter for translational motions, and 2) moving average filter for rotational motions to reject the broadband noise component (w) that affects short-term performance. The switching criteria for the proposed filters are determined by the motion patterns of mobile robots.

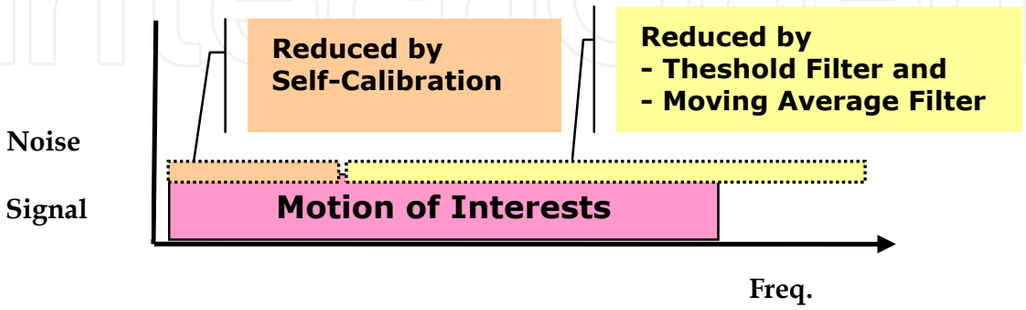

Fig. 4. The concept of de-noising

3.1 Self-calibration with least square algorithm

Our initial focus is on self-calibration of the gyro, that is, to update calibration coefficients (s and b) that have been changed somehow (temperature change, and aging, etc). During startup phase of cleaning robot, time-varying calibration coefficients of both s and b are simultaneously estimated and stored. Subsequently, when a gyro measurement is taken, it is compensated with the estimated coefficients. This means that the calibration coefficients that affect long-term performance are updated regularly so that the performance is kept consistent regardless of unpredictable changes due to aging. Ignoring the broadband noise component (w) in (1), the output of the gyro can be written

$$r_m(t) = (1+s)r(t) + b \tag{2}$$

We will often find it more convenient to express (2) as

$$r(t) = \bar{s}\, r_m(t) + \bar{b} \tag{3}$$

where $\bar{s} = \dfrac{1}{1+s}$, and . $\bar{b} = \dfrac{-b}{1+s}$.

1) Least square algorithm with heading reference

The least square algorithm presented in (Hong, 1999; Hong, 2008) is introduced to find the calibration coefficients, $\bar{s}$ and $\bar{b}$ of (3). Consider the discrete-time state equation relating yaw angle and yaw rate

$$\psi(k+1) = \psi(k) + h\ (\bar{s}\, r_m(k) + \bar{b}),\ \ k \geq 0 \tag{4}$$

where $\psi(k+1)$ is the future yaw angle, $\psi(k)$ is the initial yaw angle, and h is sample period. For any future index $n > k \geq 0$, (4) is rewritten

$$\psi(k+n) = \psi(k) + h\ \bar{s} \sum_{i=k}^{k+n-1} r_m(i) + n\,h\,\bar{b} \tag{5}$$

Taking a number of reference (true) values of yaw angle from the predetermined known motion profile (i.e., typical open-loop controlled motion profile that is assumed to be lifetime identical with precise data set provided by a factory) of robot and measurements from the gyro for increasing n and stacking the equations yields the matrix equation:

$$z = Gq \tag{6}$$

where

$$z = \begin{bmatrix} \psi(k+1) - \psi(k) \\ \psi(k+2) - \psi(k) \\ \vdots \\ \psi(k+n) - \psi(k) \end{bmatrix},\ q = \begin{bmatrix} \bar{s} \\ \bar{b} \end{bmatrix}, G = [G_1 \quad G_2]$$

and

$$G_1 = \begin{bmatrix} h\,r_m(k) \\ h\sum_{i=k}^{k+1} r_m(i) \\ \vdots \\ h\sum_{i=k}^{k+n-1} r_m(i) \end{bmatrix}, \; G_2 = \begin{bmatrix} h \\ 2h \\ \vdots \\ nh \end{bmatrix}$$

Now a least squares estimate of the scale and bias coefficients can be found by solving (6) for q

$$q = (G^T G)^{-1} G^T z \tag{7}$$

The vector q can be found as long as $G^T G$ is nonsingular, meaning that the robot should be changing rate during the calibration.

2) Evaluation

To evaluate the performance of this algorithm, some simulations are done with yaw angle reference data for some specified motion profiles. For all simulations, gyro scale and bias factors were set to s=-0.1 rad/sec/volts and b=0.1 rad/sec, corresponding to coefficient value of $\bar{s}$ =1.111, $\bar{b}$ =-0.111. Figure 5 shows the discrepancies between reference angle and gyro angle (integration of rate). The proposed least square algorithm found the coefficients of s and b with error of 4.8% and 20.26%, respectively. Subsequently, when the gyro measurements are compensated with the estimated coefficients, they show almost identical to reference data as shown in Figure 5.

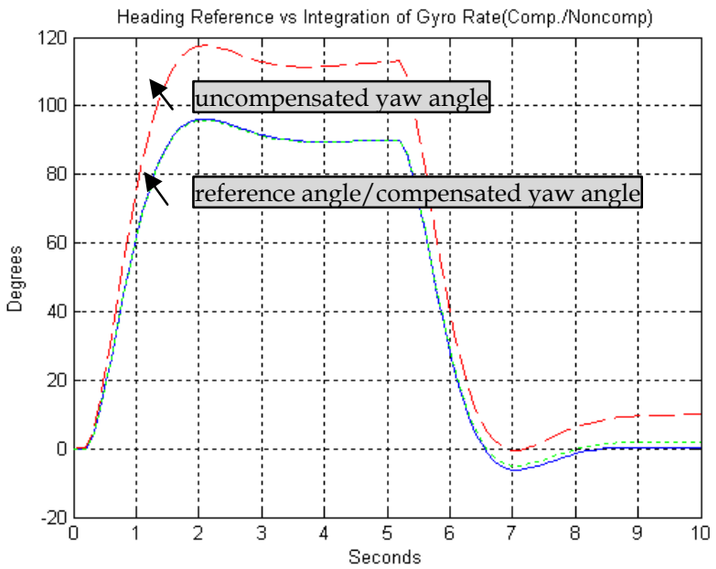

Fig. 5. Self-calibration result with least square algorithm

3.2 Identification of motion type

Before applying two different filtering schemes for short-term performance, we have to identify types of vehicle maneuver (standing/straight, steady turning, or transient). Figure 6 shows typical experimental data of XV3500 for different maneuvers. Based on the characteristics of sensor responses, the each type of vehicle maneuver is identified as:

1) If the absolute value of gyro signal lies under a certain value (with the current setting < 0.3 deg/s), the vehicle maneuver is identified as standing or straight path.
2) On the other hand, if the vehicle maneuver is not standing or straight path, and the absolute value of the error between gyro and encoder is less than a certain value (with the current setting < 5 deg/s), the vehicle maneuver is identified as steady turning.
3) If not both of maneuvers, it is considered as transient and no filter is applied to retain given edge sharpness.

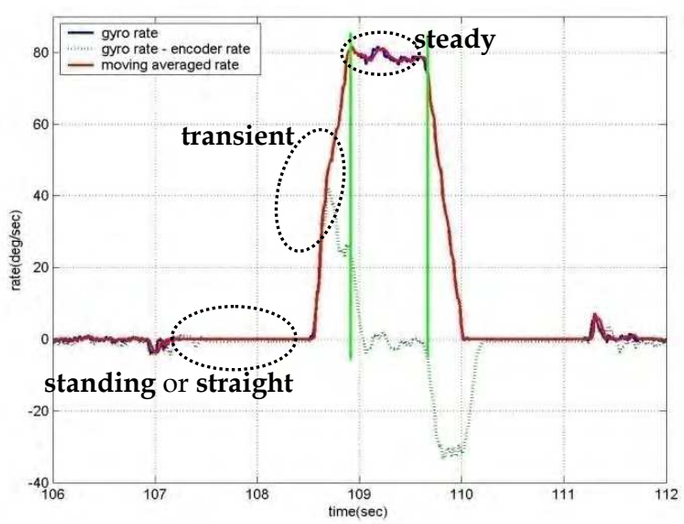

Fig. 6. Identification of typical vehicle maneuvers

3.3 Threshold filter

If the scale factor error (s) and bias (b) of the gyro are identified and compensated with the self-calibration procedures described in the section 3.1, the output of the gyro can be written as

$$r_m(t) = r(t) + d(t) + w \tag{8}$$

where d is the residual uncompensated error of the scale factor and bias. The dominant part of error d comes from the stochastic bias which is the unpredictable time-varying drift of bias, and the remaining part is the effect of uncompensated scale factor error which can be included as one source of the stochastic bias. Typically, d is modeled as a random walk as following.

$$\dot{d} = n \tag{9}$$

where n is zero-mean white noise with the spectral density Q which can be determined by analyzing the gyro output.
Figure 7(a) shows a typical output of EPSON XV3500 gyro. Note that the peak-to-peak noise is about 2 *deg/sec* dominated by the broadband noise (w). The residual error (d) is shown in Figure 7(b), which is obtained by averaging the gyro output based on an averaging time 5 min. after collecting a long term sequence of data. In this figure, the upper and lower bounds of the uncertainty are also plotted. These uncertainty bounds limit the minimum detectable signal of angular rate, and thus limit the accuracy of the heading angle calculated by integrating angular rate.

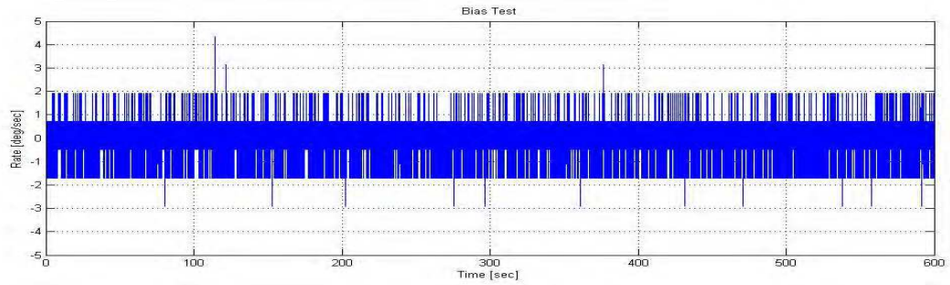

(a)

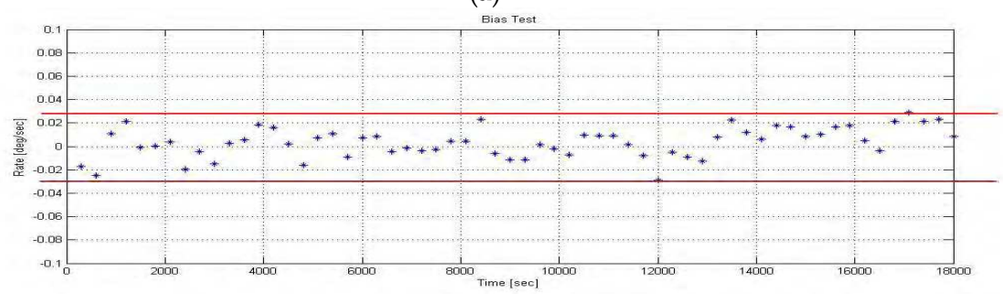

(b)

Fig. 7. Typical output of XV3500 (a) broad band noise(w), (b) residual error (d)

For the standing or straight maneuver, we implemented threshold filter. That is, the values in the gyro signal which lie under a certain threshold are filtered out and set to zero.

$$if \ |r_m| < r_{thres}, \ then \ r_m = 0 \tag{10}$$

This means that the effects of ARW or vibration are ideally eliminated when there's no turning motion. This filters out noise but of course also eliminates the gyro's capability to sense very slow turns (with the current setting < 0.3 deg/s). This has only limited significance, however, since the cleaning robot which is the application target of this study can only move with a certain minimum angular velocity (>>1 deg/s). Of course, slow changes in direction during "pure" straight path maneuver are also ignored but this is not supposed to be a major error source in the vehicle's odometry. However, it should be noted that this filter is applicable only when there's no turning motion. Figure 8(a) shows some part of rate signals captured at typical maneuvers of the platform, and the effectiveness of

proposed threshold filter can be seen in Figure 8 (b), that is zoomed in for the circled region (straight maneuvering state) of Figure 8(a).

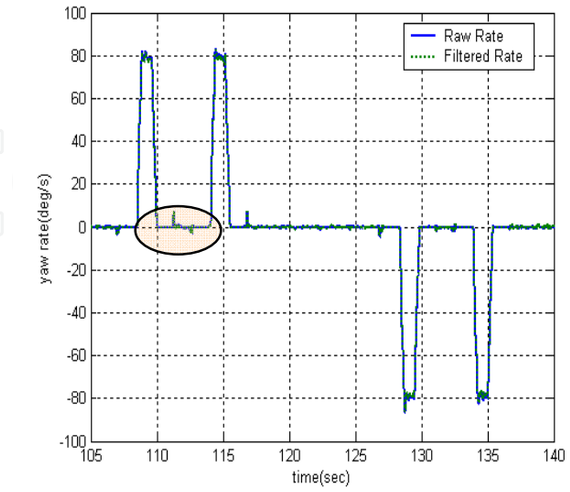

(a)

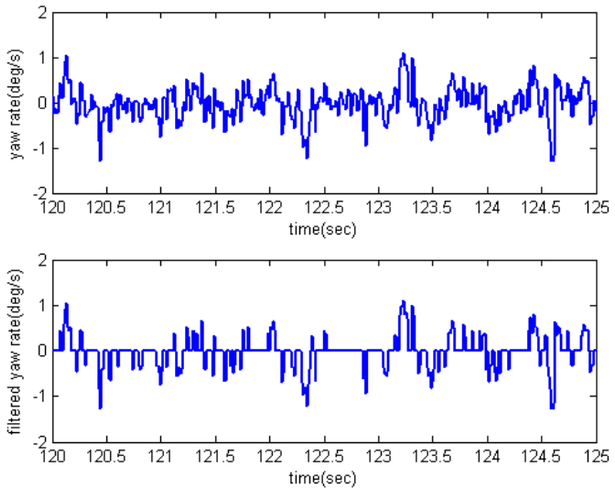

(b)

Fig. 8. Raw and filtered yaw rate signals for the straight maneuvering state

3.4 Recursive moving average filter

The moving average is the most common filter, mainly because it is the easiest digital filter to understand and use. As the name implies, the moving average filter operates by averaging a number of points from the input signal to produce each point in the output signal. As the number of points in the filter increases, the noise becomes lower; however, the edges becoming less sharp. In this study, for the optimal solution that provides the lowest noise possible for a given edge sharpness, the moving average filter is applied only when the vehicle maneuvers steady turning. Thus the given sharpness of transient motion could be retained without distortion.

For computational efficiency we perform the calculation of the mean in a recursive fashion. A recursive solution is one which depends on a previously calculated value. Suppose that at any instant k, the average of the latest n samples of a data sequence, x_i, is given by:

$$\bar{x}_k = \frac{1}{n}\sum_{i=k-n+1}^{k} x_i \tag{11}$$

Similarly, at the previous time instant, k-1, the average of the latest n samples is:

$$\bar{x}_{k-1} = \frac{1}{n}\sum_{i=k-n}^{k-1} x_i \tag{12}$$

Therefore,

$$\bar{x}_k - \bar{x}_{k-1} = \frac{1}{n}\left[\sum_{i=k-n+1}^{k} x_i - \sum_{i=k-n}^{k-1} x_i\right] = \frac{1}{n}\left[x_k - x_{k-n}\right] \tag{13}$$

which on rearrangement gives:

$$\bar{x}_k = \bar{x}_{k-1} + \frac{1}{n}\left[x_k - x_{k-n}\right] \tag{14}$$

This is known as a moving average because the average at each kth instant is based on the most recent set of n values. In other words, at any instant, a moving window of n (current setting in this study is 10) values are used to calculate the average of the data sequence (see Figure 9).

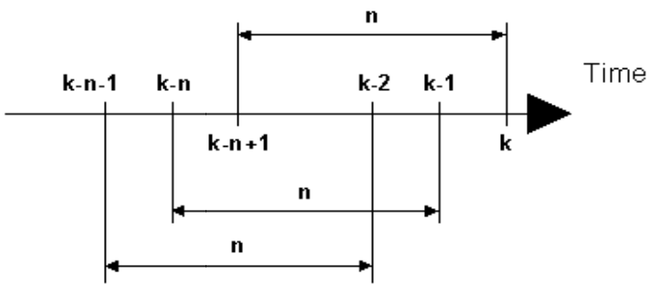

Fig. 9. Moving Window of n Data Points

4. Experimental Results

4.1 Experimental Setup

The practical technique proposed in this chapter was tested using an Epson XV3500, a low-cost MEMS gyro with 35 deg/h bias drift, and 3.7°/√hr ARW. It is mounted on the robot

platform that is a self-made conventional two-wheel differential drive with two casters (Figure 10). The robot was tested on a preprogrammed trajectory for 320 sec and self-calibration period are given for 20sec. We used the Hawk Digital system from Motion Analysis, Inc. to obtain the ground truth data of the robot heading. The robot traveled at a maximum speed of 2.0 m/s, and the reference data and XV3500 gyro measurements were acquired at sampling rates of 20Hz and 100Hz, respectively.

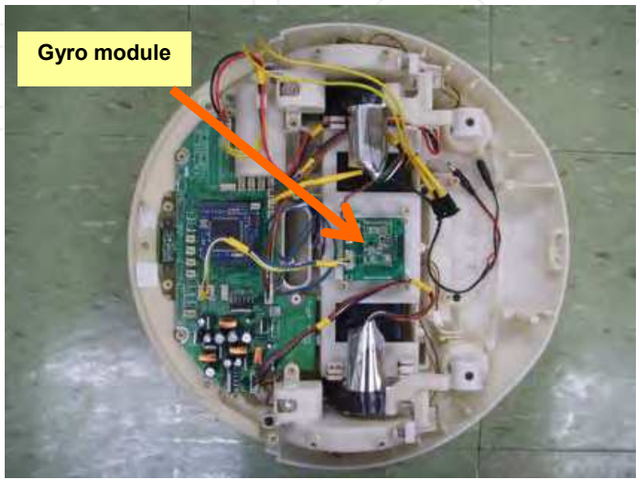

Fig. 10. Robot Platform

4.2 Results

The yaw angles correspond to preprogrammed trajectory is shown in Figure 11(a). The angle error is the mean absolute value of error between the true and the estimated value. From Figure 11(b), that is exaggerated some part of Figure 8(a), it can be seen that the error of gyro angle (pure integration of rate signal) is growing over time. It shows a fundamental limitation to any angle measurement that relies solely on pure integration of rate signal. On the other hand, after self-calibration or threshold filtering, the mean error has been reduced by 48% and 59% respectively, compared with pure integration result (shown in Figure 11(c)). This improvement, of course, is due to proper handling of major error sources that affects long-term or short-term performance when straight path maneuvering, respectively. However, both results show some drift over time. From Figure 11(d), it can be seen that the heading angle of the proposed method 1 (both self-calibration and threshold filtering) follows the true yaw angle showing little drift at all time, showing 64% error reduction. This is considered to be quite good performance for automotive grade gyros. However, it should be noted that perfect drift free heading is possible only when ARW that exists even in the turning motion is rejected. In our proposed method 1, threshold filter can reject noise components only when no rotation is applied. Figure 11(e) shows proposed method 2 that combines both threshold filter for straight maneuver and moving average filter for steady turning maneuver. It almost follows the true heading showing little drift at all time, showing 74% error reduction. All the results are summarized in Table 1 with improved bias drift estimation.

	Mean Error (deg)	Standard Deviation(deg)	Estimated Bias Drift (deg/hr)
Pure Integration	3.2645	1.8838	36
Self-Calibration	1.6774	1.7599	18
Threshold filter	1.3503	1.7144	15
Proposed 1	1.2052	1.7745	13
Proposed 2	0.8353	1.9214	9

Table 2. Mean yaw angle for each method (deg)

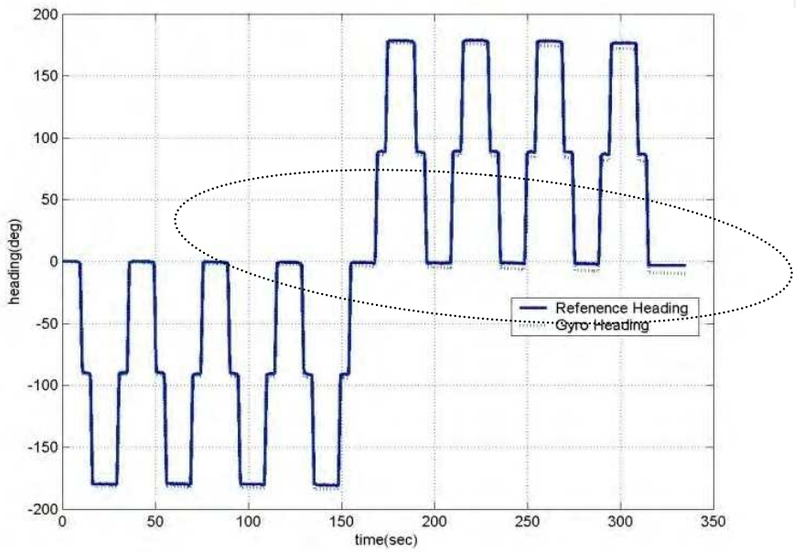

(a)

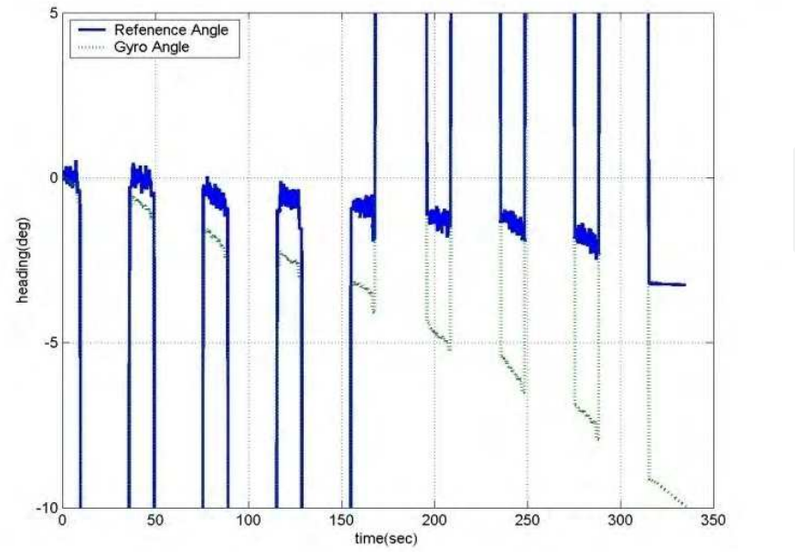

(b)

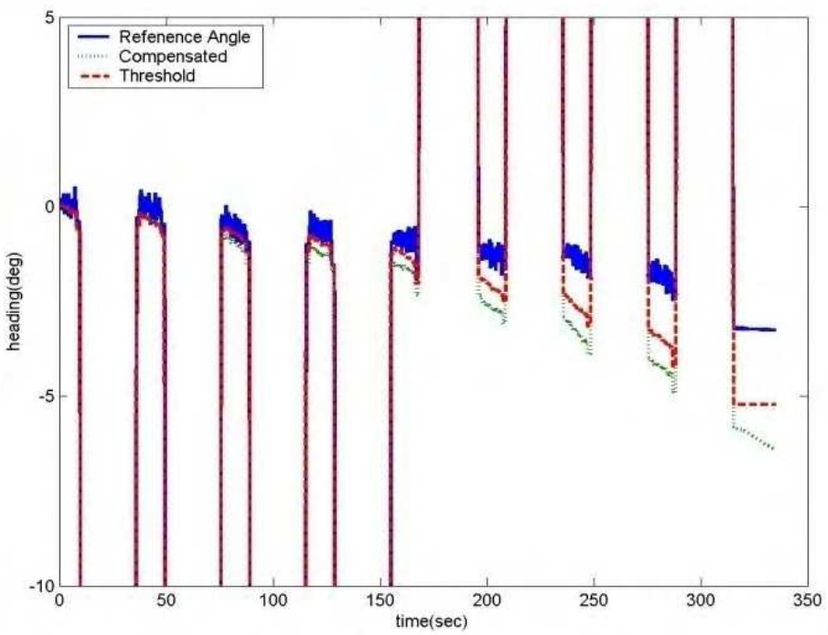
Refenence Angle
Compensated
Threshold
heading(deg)
time(sec)
5
0
-5
-10
0
50
100
150
200
250
300
350

(c)

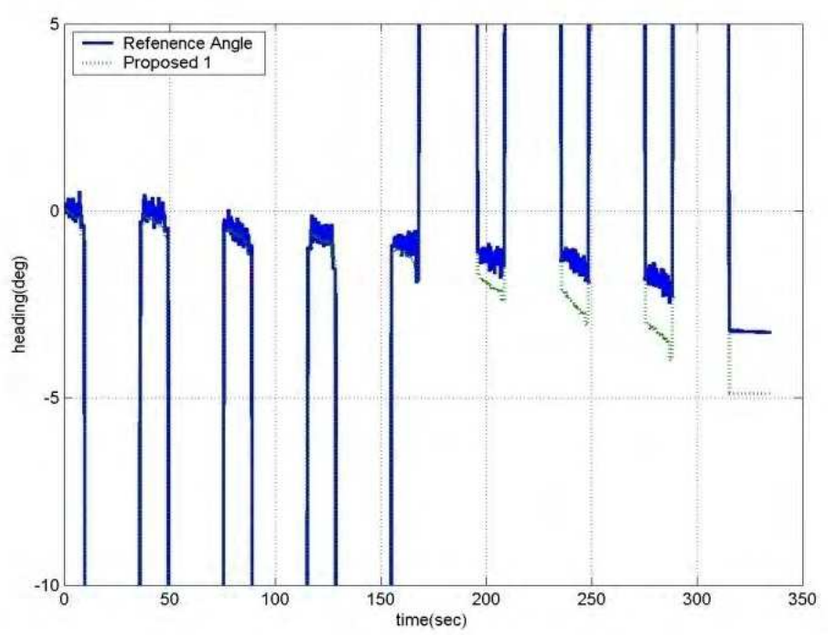
Refenence Angle
Proposed 1
heading(deg)
time(sec)
5
0
-5
-10
0
50
100
150
200
250
300
350

(d)

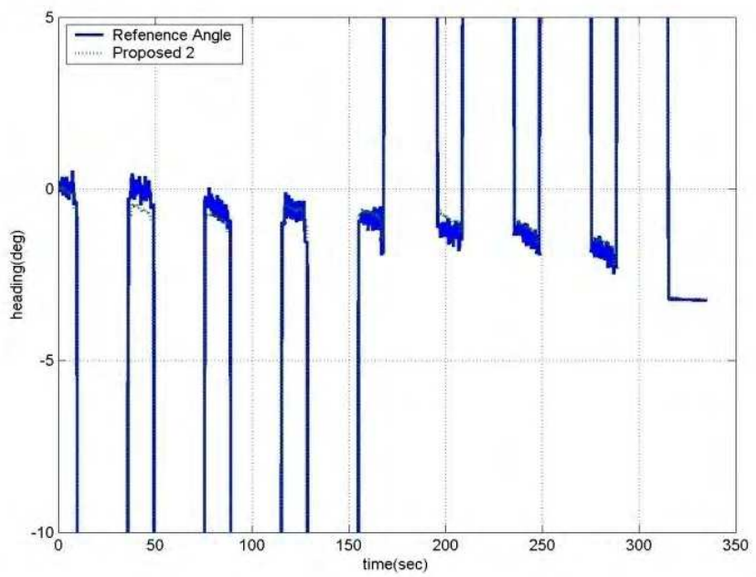

(e)

Fig. 11. Experimental results for each method

5. CONCLUSION

To achieve further minimized drift on yaw angle measurements for mobile robot, this chapter examines a simple, yet a very practical and effective filtering method that suppresses short-term broadband noise in low cost MEMS gyros. This filtering method is applied after the self-calibration procedure that is a novel algorithm developed for the long-term performance. The main idea of the proposed approach is consists of two phases; 1) threshold filter for steady or straight path maneuver, and 2) moving average filter for steady turning maneuver. However, it should be noted that no filter is applied to retain given edge sharpness for transient period. The switching criteria for the proposed filters are determined by the motion patterns of vehicle recognized via the signals from both gyro and encoder. Through this strategy, short-term errors at the gyro signal can be suppressed, and accurate yaw angles can be estimated regardless of motion status.

The proposed method that combines both threshold filter for straight maneuver and moving average filter for steady turning maneuver was evaluated through experiments with Epson XV3500 gyro showing little drift at all time (estimated bias drift as 9 deg/hr), and 74% error reduction, compared with pure integration result. This method can be extended to increase the travel distance in-between absolute position updates, and thus results in lower installation and operating costs for the whole system.

6. Acknowledgement

This work was supported by National Strategic R&D Program for Industrial Technology from Ministry of Knowledge Economy, Korea. The contents of this chapter are reorgarnized based on our previous works (Hong & Park, 2008, Hong, Moon, & Ryuh, 2009)

7. References

Epson Toyocom Corp. (2006). Angular Rate Sensor XV3500CB Data sheets, Ver. 1.0, 2006

Barbour, N. & G. Schmidt (2001). Inertial Sensor Technology Trends, *IEEE Sensors Journal*, Vol. 1, No. 4, pp.332-339

Barshan, B. & Durrant-Whyte, H. F.(1995). Inertial Navigation System for Mobile Robots, *IEEE Transactions on Robotics and Automation*, Vol. 11, No. 3, pp.328-342

Chung, H.; Ojeda, L. & Borenstein, J. (2001). Accurate Mobile Robot Dead-reckoning with a Precision-calibrated Fiber Optic Gyroscope, *IEEE Transactions on Robotics and Automation*, Vol. 17, No. 1, pp.80-84

De Cecco, M.(2003). Sensor fusion of inertial-odometric navigation as a function of the actual maneuvers of autonomous guided vehicles, *Measurement Science and Technology*, Vol. 14, pp. 643-653

Hong, S. K. (1999). Compensation of Nonlinear Thermal Bias Drift of Resonant Rate Sensor (RRS) using Fuzzy Logic, *Sensors and Actuators A-Physical*, Vol. 78, No. 2, pp.143-148

Hong, S. K. (2003). Fuzzy Logic based Closed-Loop Strapdown Attitude System for Unmanned Aerial Vehicle (UAV), *Sensors and Actuators A-Physical*, Vol. 107, No. 1, pp.109-118,

Hong, S. K. (2008a). A Fuzzy Logic based Performance Augmentation of MEMS Gyroscope, *Journal of Intelligent & Fuzzy Systems*, Vol. 19, No. 6, pp. 393-398,

Hong, S. K. & Park, S. (2008b). Minimal-Drift Heading Measurement using a MEMS Gyro for Indoor Mobile Robots, *Sensors Journal*, Vol. 8, No. 11, pp. 7287-7299

Hong, S. K.; Moon, S. & Ryuh, Y. (2009). Angle Measurements for Mobile Robots with Filtering of Short-Term in MEMS gyroscopes, in Press *Transactions of the Institute of Measurement and Control.*

Jetto, L.; Longhi, S. & Vitali, D. (1999). Localization of a wheeled mobile robot by sensor data fusion based on a fuzzy logic adapted Kalman filter, *Control Engineering Practice*, Vol. 7, pp. 763-771

Skaloud, J.; Bruton, A. M. & Schwarz, K. P. (1999). Detection and Filtering of Short-Term noise in Inertial Sensors, *Journal of the Institute of Navigation*, Vol. 46, No. 2, pp. 97-107

Stilwell, D.J.; Wick, C.E. & Bishop, B.E. (2001). Small Inertial Sensors for a Miniature Autonomous Underwater Vehicle, *Proc. of IEEE International Conference on Control Applications,* pp. 841—846, Sept. 2001 , Mexico

Sun, F.; Luo, C. & Nie, Q. (2005). Research on Modeling and Compensation Method of Fiber Optic Gyro' Random Error, *Proc. of IEEE Conference on Mechatronics and Automation*, pp. 461—465, July 2005, Canada

Titterton, D. H. & Weston, J.L. (2004). Strapdown inertial navigation technology-2nd Edition, IEE Radar, Sonar, Navigation and Avionics Series 17,

Yazdi, N.; Ayazi, F. & Najafi, K. (1998). Micromachined Inertial Sensors, *Proc. IEEE*, pp.1640-1659

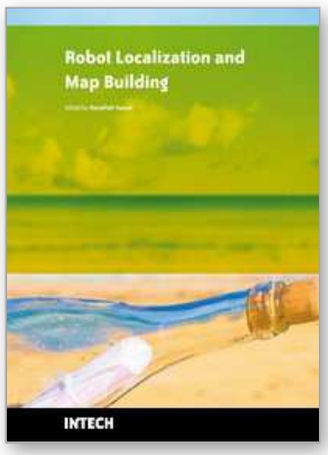

Robot Localization and Map Building

Edited by Hanafiah Yussof

ISBN 978-953-7619-83-1
Hard cover, 578 pages
Publisher InTech
Published online 01, March, 2010
Published in print edition March, 2010

Localization and mapping are the essence of successful navigation in mobile platform technology. Localization is a fundamental task in order to achieve high levels of autonomy in robot navigation and robustness in vehicle positioning. Robot localization and mapping is commonly related to cartography, combining science, technique and computation to build a trajectory map that reality can be modelled in ways that communicate spatial information effectively. This book describes comprehensive introduction, theories and applications related to localization, positioning and map building in mobile robot and autonomous vehicle platforms. It is organized in twenty seven chapters. Each chapter is rich with different degrees of details and approaches, supported by unique and actual resources that make it possible for readers to explore and learn the up to date knowledge in robot navigation technology. Understanding the theory and principles described in this book requires a multidisciplinary background of robotics, nonlinear system, sensor network, network engineering, computer science, physics, etc.

InTech Europe
University Campus STeP Ri
Slavka Krautzeka 83/A
51000 Rijeka, Croatia
Phone: +385 (51) 770 447
Fax: +385 (51) 686 166
www.intechopen.com

InTech China
Unit 405, Office Block, Hotel Equatorial Shanghai
No.65, Yan An Road (West), Shanghai, 200040, China
中国上海市延安西路65号上海国际贵都大饭店办公楼405单元
Phone: +86-21-62489820
Fax: +86-21-62489821

IntechOpen